JOURNAL OF GEOPHYSICAL RESEARCH, VOL. 107, NO. D22, 4637, doi:10.1029/2001JD000736, 2002

January and July regional climate simulation over South America

M. Nicolini[1] and P. Salio[1]
Departamento de Ciencias de la Atmósfera y los Océanos, Ciudad Universitaria, Buenos Aires, Argentina

J. J. Katzfey and J. L. McGregor
Division of Atmospheric Research CSIRO, Victoria, Australia

A. C. Saulo[1]
Departamento de Ciencias de la Atmósfera y los Océanos, Ciudad Universitaria, Buenos Aires, Argentina

Received 16 April 2001; revised 4 October 2001; accepted 11 October 2001; published 22 November 2002.

[1] This work presents results, over the South American region, from the CSIRO Division of Atmospheric Research limited area model (DARLAM) and from the nine-level general circulation model (GCM) of CSIRO (CSIRO Mk 2), within which it was nested in a one-way mode. Ten separate 30-day DARLAM simulations were performed for both January and July with a resolution of 125 km and were averaged to obtain a climatology for those months. This paper presents for the first time simulations of the January South American climate using a limited area model; previous similar studies simulated only the July climate. The goal of this study was to examine the capability of the CSIRO Mk 2 - DARLAM nested modeling system for simulating the climate in the South American region. Further, it was desired to investigate whether the higher resolution of DARLAM improves the simulated climate over various subregions, compared with the GCM and observations. With this purpose, a representative set of variables was analyzed and statistically compared. Overall, the fields simulated by the nesting system provide a better representation of the South American climate than the GCM. In particular, significant improvements are found in the nested model climatology for near-surface temperature and mean sea level pressure. Comparison of the January and July simulations shows a better wintertime performance. Some significant summertime features, like the Bolivian High, are reasonably well simulated by DARLAM, but not by the GCM. *INDEX TERMS:* 3309 Meteorology and Atmospheric Dynamics: Climatology (1620); 1620 Global Change: Climate dynamics (3309); 3337 Meteorology and Atmospheric Dynamics: Numerical modeling and data assimilation; 3354 Meteorology and Atmospheric Dynamics: Precipitation (1854); *KEYWORDS:* Regional climate modeling, South America climate, model validation

Citation: Nicolini, M., P. Salio, J. J Katzfey, J. L. McGregor, and A. C. Saulo, January and July regional climate simulation over South America, *J. Geophys. Res.*, *107*(D22), 4637, doi:10.1029/2001JD000736, 2002.

1. Introduction

[2] General circulation models (GCMs) provide a realistic contribution to the simulation of current and future climate but are not capable of resolving the smaller-scale circulation characteristics that are important for a correct regional climate simulation. Limited area models (LAMs) nested within global climate models, or nested within data analyses, are capable of representing in detail the characteristics of the orography, vegetation, and land use [e.g., *McGregor*, 1997], and therefore it is possible to obtain a much more detailed representation of the climate characteristics of the region. The GCM provides the larger-scale forcing through the borders.

[3] A number of regional climate models have been applied in multiple simulations during January and July over different regions around the world; examples include the western United States [*Dickinson et al.*, 1989; *Giorgi*, 1990], Australia [*McGregor and Walsh*, 1993; *Walsh and McGregor*, 1995], New Zealand [*Renwick et al.*, 1998], Antarctica [*Walsh and McGregor*, 1996], Europe [*Giorgi et al.*, 1990; *Giorgi and Marinucci*, 1991, 1996a, 1996b], and South Africa [*Joubert et al.*, 1999]. Various climate change scenarios have been simulated at the regional scale over the United States [*Giorgi et al.*, 1994], Europe [*Giorgi et al.*,1992], and Australia [*McGregor and Walsh*, 1994]. Simulation of the regional climate by GCMs, in particular regarding precipitation, is not completely reliable due to the low resolution of these models. This limitation justifies the need to increase model resolution to represent those effects

[1]Also at Centro de Investigaciones del Mar y la Atmósfera, CONICET-UBA, Buenos Aires, Argentina.

0148-0227/02/2001JD000736

of subgrid scales forced by the topography and the complex curvature of continental coasts. *Labraga* [1997] and *Carril et al.* [1997] address some of these problems comparing the performance of different models with the objective to study climate change scenarios for South America. *Chou et al.* [2000] showed results from a dry and wet season month (August and November, respectively) in simulations over South America for 1997 using the regional Eta model; the model used the NCEP analysis as initial conditions; lateral boundary conditions were provided by the Centro de Previsão de Tempo e Estudos Climáticos-Center for Ocean-Land Atmosphere Studies (CPTEC/COLA) GCM. The improvement on the forecast with the regional model was significant during the dry month, whereas during the wet month the regional model underestimated the precipitation.

[4] This work presents results from the 9-level GCM of CSIRO (CSIRO Mk 2) and the CSIRO Division of Atmospheric Research limited area model (DARLAM) nested in the CSIRO Mk 2 GCM output over the South American region. Ten separate 30-day simulations have been performed for both January and July with a resolution of 125 km and have been averaged to obtain a climatology for those months. We simulate for the first time January South American climate using a LAM; previous LAM studies simulate only the July climate [*Menendez et al.*, 2000]. Section 2 describes the characteristics of the model. Statistical methodology and observational data used for evaluation are presented in section 3. These statistics have been evaluated for selected regions in order to test the performance of the models in different geographical conditions. In section 4, large-scale patterns and both driving GCM and nested model system performance are analyzed, and results are discussed in view of the uncertainty in the data sets used for validation. Finally conclusions are summarized in section 5.

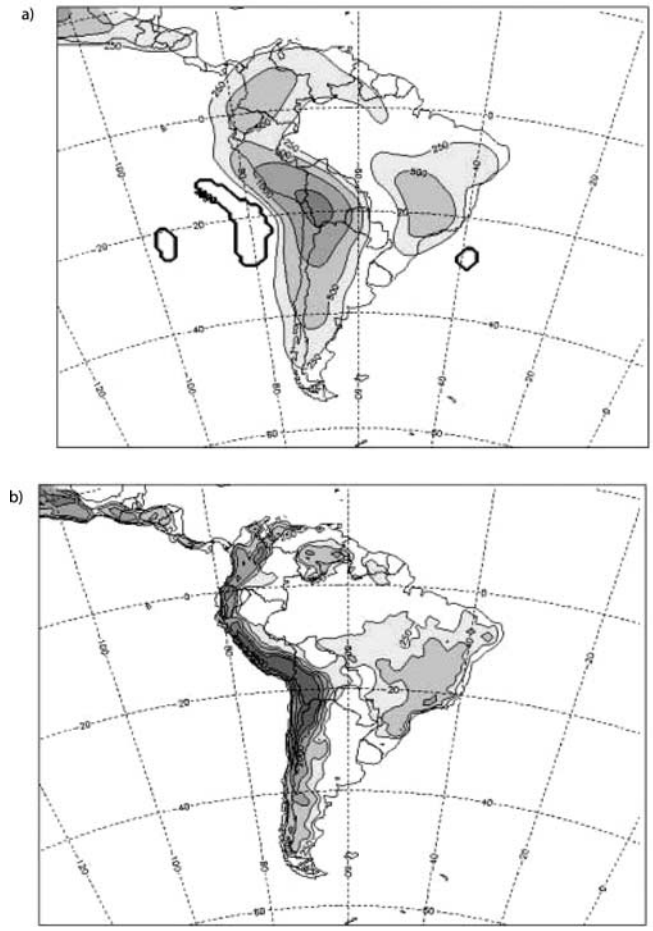

Figure 1. (a) CSIRO 9 Mk 2 orography and (b) DARLAM model domain for the present simulations. Orography is shaded, contours interval are 250, 500, 1000, 2000, and 3000 m.

2. Nested Model Description

[5] DARLAM is a two-time level, semi-implicit, hydrostatic primitive equations model, developed for both mesoscale studies and climate change experiments. The model uses an Arakawa staggered C grid and semi–Lagrangian horizontal advection with bicubic spatial interpolation [*McGregor*, 1987; *Walsh and McGregor*, 1995]. A one-way nesting strategy is adopted here, with lateral boundary conditions and sea surface temperatures (SSTs) specified 12 hourly by the CSIRO Mk 2 GCM [*Watterson et al.*, 1995]. The GCM was run with a slab ocean with prescribed ocean heat transport.

[6] At each time step, the outermost DARLAM boundary rows are relaxed toward the interpolated values provided by the GCM, using the nesting procedure of *Davies* [1976], but with exponentially decreasing weights. Boundary conditions are provided by ten Januarys and ten Julys from the CSIRO Mk 2 control simulations.

[7] DARLAM uses the same nine vertical level structure as the CSIRO Mk 2 GCM on the 125 km horizontal resolution Lambert-conformal domain shown in Figure 1b. The models utilize the sigma coordinate in the vertical with a nonuniform spacing. Although the vertical resolution is relatively coarse nowadays, it was considered desirable to keep the vertical resolution the same as the GCM in order to more clearly demonstrate the impact of horizontal resolution and nesting.

[8] The LAM incorporates a comprehensive set of physical parameterizations, which are essentially the same as those of the GCM. The cumulus convection scheme adopted for these experiments is a modified version of the *Arakawa* [1972] scheme and uses a mass flux closure. Several other convection schemes have been tested in earlier (unpublished) sensitivity tests. The convective scheme adopted here perfomed well over numerous multiple single-month sensitivity tests. Both models use an updated version of the scheme described by *Walsh and McGregor* [1995] for soil moisture (two layers) and soil temperature (three layers). The updated scheme has vegetation data, including soil and vegetation type, physical characteristics, and albedo derived from the Simple Biosphere Model (SIB) data [*Dorman and Sellers*, 1989]. The U.S. Navy 5 min orography was averaged to the LAM grid boxes. The boundary layer treatment follows *Louis* [1979].

[9] The R21 spectral resolution of CSIRO Mk 2 (~500 km Gaussian grid resolution) results in a very smoothed representation of orographic features over South America (Figure 1a). The Andes is narrow and steep, and maximum altitudes are underestimated. DARLAM, with a horizontal

Figure 2. Map showing the regions used to calculate comparative statistics between DARLAM, CSIRO Mk 2, and the observations in the Tables. Dark shading is Mountain region, medium shading over Brazil is Amazonia, medium shading over Argentina is RP Basin, and light shading is B Plateau.

resolution of 125 km, provides a more realistic representation of regional orographic features over South America (Figure 1b).

3. Statistical Methodology and Observational Data

[10] *Katz* [1992] has discussed different problems and techniques related to statistical verification of model output versus observational data. Standard statistical measures used herein to assess the quality of the nested system in simulating present-day climate are the following:

1. Pattern correlation (ρ) of two spatial fields is defined as the correlation of a series of data points X_i from one field with corresponding values O_i from the other field:

$$\rho = \frac{\sum (X_i - \overline{X})(O_i - \overline{O})}{\left[\sum (X_i - \overline{X})^2\right]^{1/2}\left[\sum (O_i - \overline{O})^2\right]^{1/2}}, \qquad (1)$$

where $\overline{X}$ is the mean of 10 years model fields X_i and $\overline{O}$ is the mean of the observations O_i described below. In this paper, model fields X_i and observations O_i are both interpolated to the LAM grid, using a bicubic interpolation technique, which is adequate given the smooth nature of the monthly averaged fields.

2. The root mean square error (RMS) is defined as

$$\mathrm{RMS} = \left[\frac{\sum (X_i - O_i)^2}{N}\right]^{1/2}, \qquad (2)$$

where N is the number of points over which the sum is taken.

3. The mean spatial deviation (bias) is defined as

$$\mathrm{bias} = \left[\frac{\sum (X_i - O_i)}{N}\right]. \qquad (3)$$

As a first step, the statistics have been calculated over the DARLAM domain, first including points only over the sea and then only over the continent. To further clarify the analysis of results, the DARLAM continental domain has been divided into several regions depicted in Figure 2. A topographic criterion has been used to identify subregions.

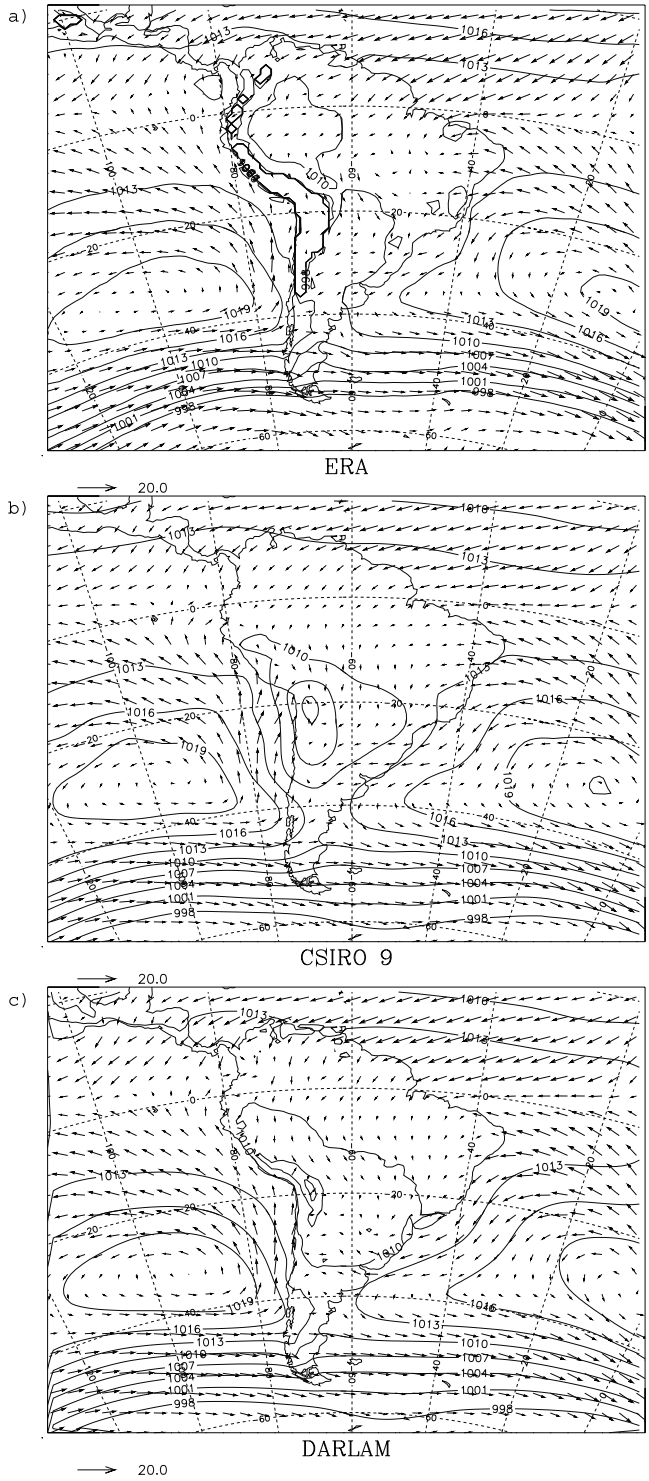

Figure 3. January MSLP (hPa) and wind vectors at the 0.98 sigma level for (a) ERA, (b) CSIRO Mk 2, and (c) DARLAM. Contour interval is 3 hPa.

Table 1. Spatial Pattern Correlation, Root Mean Square Error, and Spatial Bias of January MSLP for CSIRO Mk 2, and DARLAM[a]

		Pattern Correlation		RMS, hPa		Bias, hPa	
	N	GCM	DARLAM	GCM	DARLAM	GCM	DARLAM
Sea	7326	0.96	0.90	2.86	2.60	1.20	0.81
Continent	1687	0.21	0.27	2.54	2.39	−0.19	−0.58
Amazonia	534	0.71	0.83	0.87	0.53	0.58	0.09
RP Basin	193	0.82	0.70	1.20	1.12	0.73	−0.23
B Plateau	382	0.76	0.60	0.71	1.26	0.13	−0.89

[a]RMS, root mean square; *N* is the number of DARLAM grid points; the subregions are defined in section 2.

Mountainous areas have been included in two main subregions: the first area is representative of the Andes (Mountain), while the second is representative of the Brazilian Highlands (B Plateau). The two main river basins in South America are also defined as subregions: the Del Plata Basin (RP) and Amazon Basin (Amazonia).

[11] We note that in comparing simulations of precipitation, it is desirable to use a quantity having an aproximately normal distribution, in order to avoid biases in the analysis toward high or low rainfall values. For transforming the highly skewed spatial distribution of precipitation to a more normal distribution, *Stidd* [1953] proposed the use of the cube root of precipitation, denoted here by $P^{1/3}$.

[12] The evaluation of the quality of the simulations depends on the reliability of the observational data against which they are compared. *Xie and Arkin* [1997] mean daily precipitation rate data with an horizontal resolution of 2.5° × 2.5° are used to calculate the statistics. In spite of lower resolution compared to some other data, this data set is preferred because it also includes satellite estimations and modeled values. This assures a better representation over the ocean regions. European Centre Medium Weather Forecast (ECMWF) reanalyses (ERA, data during the period 1982–1993 with horizontal resolution of 1.125° in longitude and a Gaussian grid in latitude) are used to validate the fields of mean sea level pressure (MSLP), temperature at the lowest sigma level, meridional, and zonal components of the wind [*Gibson et al.*, 1996, 1997]. A 16-point bicubic interpolation technique is used to interpolate these fields to the DARLAM grid.

4. Results

4.1. Mean Sea Level Pressure

4.1.1. January

[13] Mean sea level pressure over the South American continent during January (Figure 3a) is dominated by a thermal-orographic low and two subtropical anticyclones located east and west of the continent over the oceans [*Schwerdtfeger*, 1976]. The depression is clearly localized between (20°S and 30°S) and between 55°W and 65°W, over the relatively dry terrain to the east of the Andes. The South Pacific subtropical anticyclone is centered around 32°S, 100°W, slightly further south than the corresponding South Atlantic anticyclone. The western border of the Atlantic anticyclone is perturbed by cyclogenesis episodes that make it more difficult to locate its maximum over the coast [*Minetti and Vargas*, 1983].

[14] The GCM simulates the characteristics of the surface pressure for January (Figure 3b) reasonably well, in spite of a slight shift in the position of the depression over the continent towards the west (20°S, 68°W). The simulated low is deeper than that observed in the ERA field. The circumpolar trough is more weakly represented with around 6 hPa difference. Subtropical anticyclones are correctly simulated by CSIRO Mk 2, in spite of a slight overestimation of the Atlantic anticyclone intensity compared with the observed. The largest differences between CSIRO Mk 2 and DARLAM (Figure 3c) are found over the continent where the depression in DARLAM is extended more toward the east, similar to ERA.

[15] A comparison of CSIRO Mk 2 and DARLAM statistics in the selected subregions is presented in Table 1. The model statistics are fairly similar for MSLP. DARLAM has better pattern correlations over Amazonia but is inferior over the RP Basin. The DARLAM RMS errors are also smaller over Amazonia. Although the DARLAM biases are slightly larger over the continent as a whole, they are smaller over the sea, Amazonia, and the RP Basin regions.

4.1.2. July

[16] Figure 4a depicts the July MSLP. A displacement of the subtropical anticyclonic belt toward lower latitudes, with respect to the January position, is evident. This shift is coincident with an expansion of the westerlies over the Patagonia region. The two anticyclonic cells have a similar latitudinal extension, while the Atlantic center is stronger. The Atlantic subtropical anticyclone extends over the continent for this month.

[17] Figure 4b shows the problems CSIRO Mk 2 had in simulating the Pacific subtropical anticyclone correctly, while DARLAM reproduces its position quite well even if slightly weaker (Figure 4c). The ridging over central Argentina and Uruguay is clearly represented by both models. In contrast with the January results, the circumpolar trough is correctly represented by the two models, both in intensity and location.

[18] Over the sea and continent subregions, the statistics for the two models are quite similar (Table 2); the GCM has a slightly smaller bias over the sea and slightly better pattern correlation over the continent; DARLAM has slightly smaller RMS error and bias over the continent. However, DARLAM produces a pronounced improvement compared to the GCM for all three statistics over Amazonia and the RP Basin.

4.2. Temperature

4.2.1. January

[19] Figure 5a shows the January temperature field interpolated to the lowest DARLAM sigma level (∼170 m) from ERA. *Schwerdtfeger* [1976] has described the main charac-

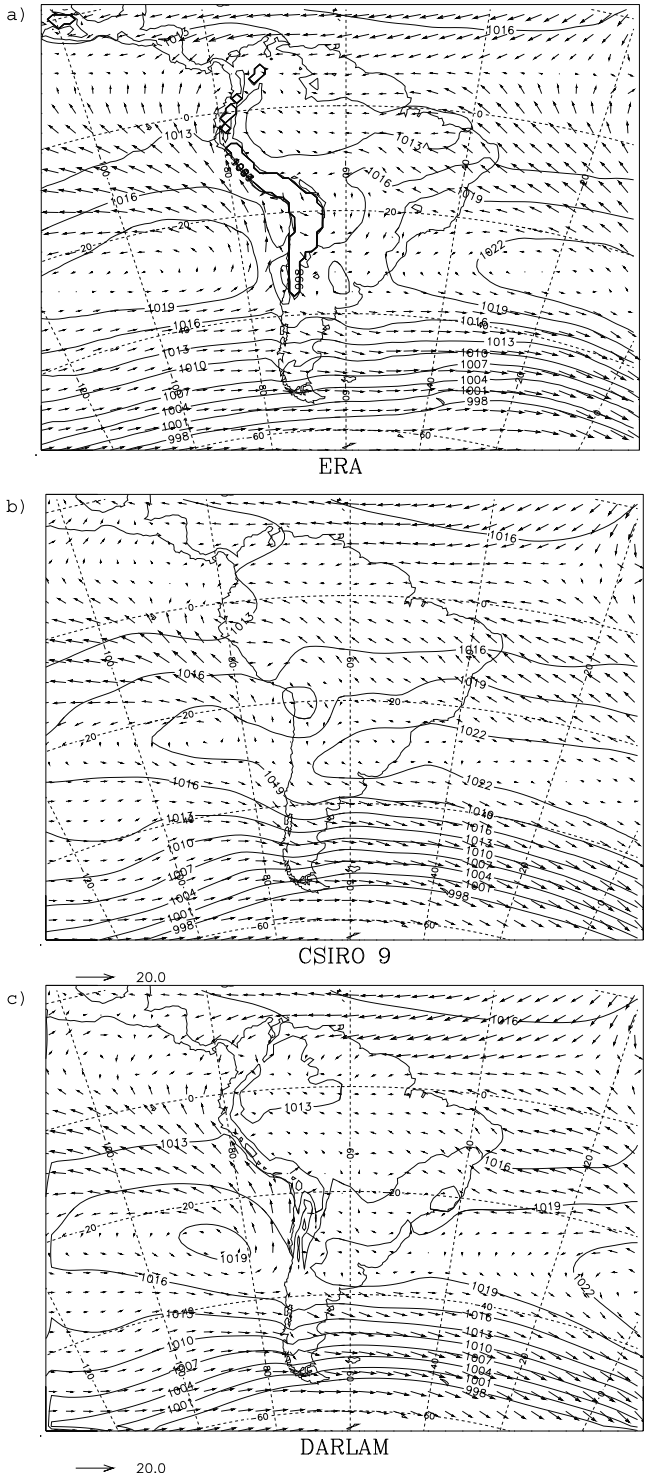

Figure 4. Same as in Figure 3, but for July.

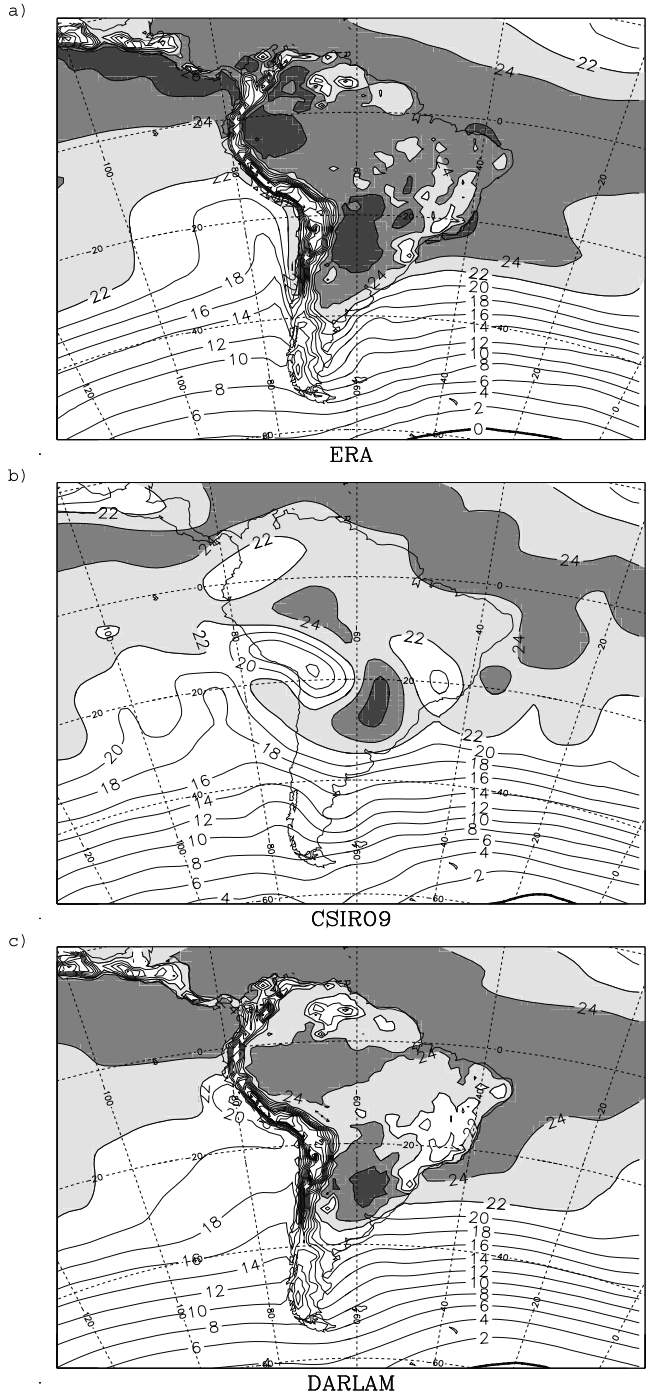

Figure 5. January temperature (°C) at 0.98 sigma level for (a) ERA, (b) CSIRO Mk 2, and (c) DARLAM. Contour interval is 2°C and temperatures higher than 22°C are shaded.

Table 2. Same as for Table 1, but for July

		Pattern Correlation		RMS, hPa		Bias, hPa	
	N	GCM	DARLAM	GCM	DARLAM	GCM	DARLAM
Sea	7326	0.95	0.95	2.39	2.42	−0.25	−0.71
Continent	1687	0.87	0.80	2.11	1.87	1.08	−0.54
Amazonia	534	0.57	0.79	1.41	0.46	1.21	0.26
RP Basin	193	0.65	0.83	3.86	1.08	3.63	0.60
B Plateau	382	0.90	0.95	1.76	1.02	1.41	−0.56

Table 3. Spatial Pattern Correlation, Root Mean Square Error, and Overall Spatial Bias January Temperature at the Lowest Model Level for CSIRO Mk 2 and DARLAM, Compared to ERA[a]

		Pattern Correlation		RMS, °C		Bias, °C	
	N	GCM	DARLAM	GCM	DARLAM	GCM	DARLAM
Sea	7326	0.99	0.99	1.20	0.894	−0.42	−0.05
Continent	1687	0.73	0.98	3.65	2.00	−0.91	−1.72
Amazonia	534	−0.10	0.64	2.57	1.68	−2.17	−1.51
Mountain	500	0.58	0.99	5.50	2.42	1.54	−2.15
RP Basin	193	0.73	0.81	2.67	1.57	−2.11	−1.06
B Plateau	382	0.28	0.82	2.18	2.04	−1.46	−1.89

[a]RMS, root mean square; *N* is the number of DARLAM grid points; the subregions are defined in section 2.

teristics of this field during January. A maximum temperature, with values higher than 26°C, is centered over the Paraguayan Chaco approximately at 22°S, 60°W. CSIRO Mk 2 and DARLAM (Figures 5b and 5c, respectively) simulate correctly the intensity of the maximum temperature, positioned in both cases at 26°S, 56°W, slightly shifted southeast from its observed position. Related to this maximum, the ERA field displays a high temperature tongue along the 60°W meridian that penetrates southwards to northern Patagonia. This tongue is weakly suggested by the CSIRO Mk 2 fields, while DARLAM is better able to reproduce the ERA pattern, as a result of its improved topography resolution.

[20] Over Brazil, the main factors controlling the distribution of temperatures are the height and the tropical location. The Brazilian highlands region depicts minimum temperature values due to a terrain elevation that exceeds 1000 m in some places. The CSIRO Mk 2 simulation is quite similar to the observed, although the better resolution of DARLAM improves the location of the minima.

[21] In the Amazon region, both the GCM and DARLAM simulate lower temperature than observed; the CSIRO Mk 2 discrepancy is larger than DARLAM. In the coast of Venezuela and of Guyana, higher elevations along with the trade winds are a modifying climate factor and generate cooler temperatures. This feature is apparent in the DARLAM field but is only weakly simulated by CSIRO Mk 2.

[22] DARLAM produces a pronounced improvement over all continental areas and especially over mountain areas (Table 3) and Amazonia. It should be mentioned that there is uncertainty in the data over Amazonia. A pattern correlation of 0.52 between ERA and NCEP data sets (National Centers for Environmental Prediction Reanalysis [*Kalnay et al.*, 1996]) was calculated for the same period; this behavior reduces confidence in the reanalyses over this region.

[23] Both models show a tendency to produce lower temperatures over the whole region, with biases up to −2°C; CSIRO Mk 2 artificially reduces the bias over the mountains due to its lower orography. Both models also have a tendency to produce a negative moisture bias of ∼1 g kg^{-1} over the Amazon region (not shown); this behavior also occurs for July.

4.2.2. July

[24] During July the ERA temperature field (Figure 6a) shows a simpler pattern than during January and in general the dominant north-south gradient is apparent. However, it is important to note the influence of the terrain elevation in

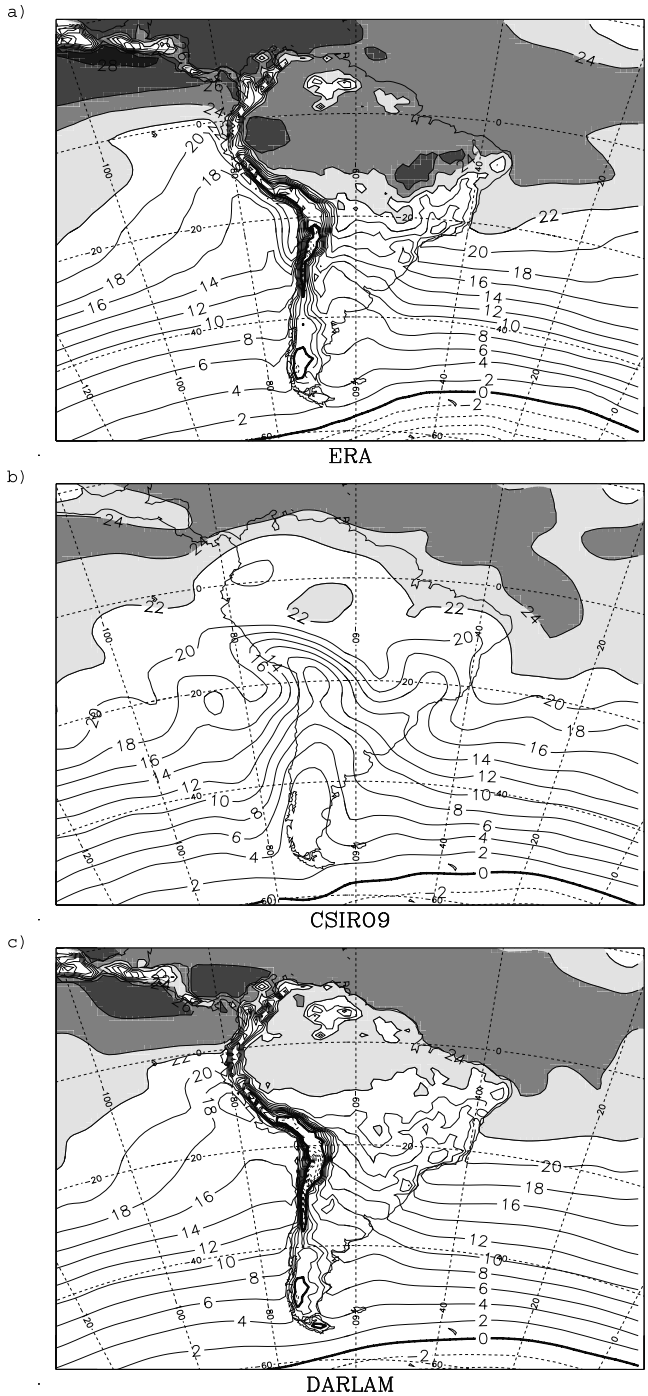

Figure 6. Same as in Figure 5, but for July.

Table 4. Same as for Table 3, but for July

		Pattern Correlation		RMS, °C		Bias, °C	
	N	GCM	DARLAM	GCM	DARLAM	GCM	DARLAM
Sea	7326	0.99	0.996	1.53	1.15	−0.09	0.19
Continent	1687	0.91	0.98	3.95	2.81	−2.13	−2.37
Amazonia	534	0.22	0.66	3.69	2.43	−3.49	−2.35
Mountain	500	0.83	0.97	4.97	3.22	−0.02	−2.47
RP Basin	193	0.95	0.98	2.76	1.52	−2.29	−1.05
B Plateau	382	0.83	0.95	3.50	3.40	−2.94	−3.19

the spatial temperature distribution, both along the Andes and over other orographic features. The nested system (Figure 6c) represents the Andes and the Brazilian highlands with better detail than the GCM (Figure 6b), even if it is colder than the observed field.

[25] The pattern correlations (Table 4) show a better performance of CSIRO Mk 2 in July than in January, likely related to the larger north-south gradient; however, DARLAM is still superior to CSIRO Mk 2 in July. Again, as in January, the uncertainty in data over Amazonia is large, and there is a tendency for the models to simulate lower temperatures over the region. Note that the biases and RMS values are larger in July than for January.

4.3. Average Daily Precipitation

[26] Precipitation is one of the most difficult variables to simulate. An additional difficulty is related to the large number and variety of precipitation regimes that develop in South America. Most of them are associated with regional circulation patterns and topographic characteristics.

[27] A thorough description of the main precipitation regimes from rain gauge observational data is included by *Schwerdtfeger* [1976]. A brief characterization of these regimes is also possible from the *Xie and Arkin* [1997] fields for January and July (Figures 7a and 8a, respectively). Figures 7b and 7c show the CSIRO Mk 2 and DARLAM average daily precipitation during January, respectively, while Figures 8b and 8c show the same during July.

[28] An important arid and semi-arid corridor is present in January, oriented northwest to southeast from southern Ecuador, along the Peruvian coast through central Chile and western Argentina up to central Patagonia (see the 2 mm d^{-1} contour in Figure 7a). Both CSIRO Mk 2 and DARLAM show a good representation of this arid region with a broader extension over the continent in the CSIRO Mk 2 field due to its lower resolution of the Andes. However, DARLAM develops a maximum of precipitation over northwestern Argentina during January at variance with the observed field. This precipitation maximum is related to excessive orographic precipitation in DARLAM.

[29] A characteristic orographic precipitation region depicted by the *Xie and Arkin* [1997] data is located over the Chilean coast, extending from Cape Horn up to around 35°S during both months. It is notable that due to the improvement in orographic representation, DARLAM correctly simulates this region in position and intensity during both months, with a slight tendency for reduced values during January.

[30] A tropical precipitation regime (with a maximum during January) dominates the eastern slope of the Andes in central and southern Peru, Bolivia, and northwestern Argentina. This maximum is suggested by CSIRO Mk 2, despite its limitations in orographic representation; the nesting system is able to slightly represent it. However, a dry season (July) minimum is well defined by both CSIRO Mk 2 and DARLAM (Figures 8b and 8c, respectively).

[31] The annual displacement of the intertropical convergence zone (ITCZ) along the northern and northeastern coast of South America is a clear feature of the precipitation in that region. DARLAM performs much better than CSIRO Mk 2 in ITCZ intensity and location and reproduces correctly the ITCZ displacement to the north during July.

[32] The South American Convergence Zone (SACZ) is a predominant feature during summer which has been studied by several authors (see *Liebmann et al.* [1999], *Nogués-Paegle and Mo* [1997], among others), and that is represented by a slight extension toward the southeast of the maximum that intersects the coastline at 25°S. DARLAM simulates SACZ, although it is shifted to the north of its observed position.

[33] Over Amazonia, maximum precipitation during summer is underestimated by both CSIRO Mk 2 and DARLAM. On the contrary, an excess of precipitation is noticed over northeastern Brazil. This behavior could be due to not enough compensating subsidence over this area linked to a weakened precipitation over Amazonia. This model failure in precipitation is discussed in section 4.5 in relation to heat sources and low-level circulation. Excessive precipitation is also produced over the mountain areas, confirming similar results for other regions (see *Jenkins and Barron* [1997], *McGregor and Walsh* [1994], *Giorgi et al.* [1994], among others).

[34] Tables 5 and 6 show statistics related to precipitation fields. It is possible to observe a better performance over Del Plata Basin in January and July. Other regions produce statistics similar to the GCM.

4.4. High-Level Winds

[35] The ERA wind field (sigma = 0.1 level, i.e., ∼100 hPa) during January (Figure 9a) shows the presence of an anticyclonic circulation over the Bolivian Plateau called the Bolivian High, approximately centered at 18°S, 65°W, and a trough immediately to the east of Brazil. The Bolivian High is mainly caused by convective latent heat release in middle levels over Amazonia [*Lenters and Cook*, 1997; *Figueroa et al.*, 1995], whereas the trough is partly explained by this mechanism but is also influenced by the condensational heat source and related divergence zone positioned over Africa [*Gandu and Silva Dias*, 1998]. The subtropical jet is located around 50°S with two maxima:

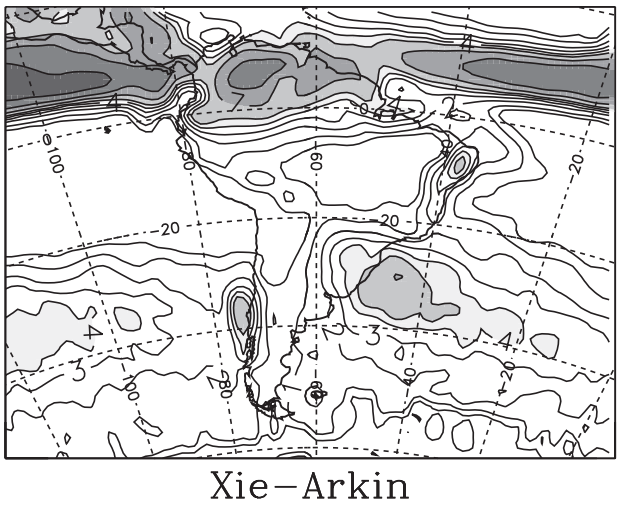

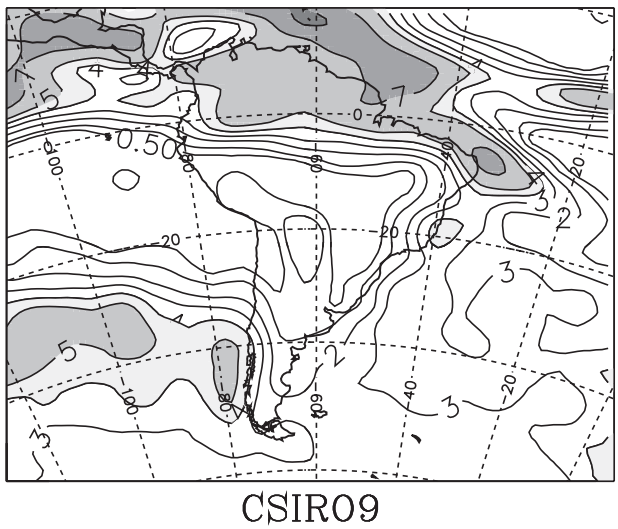

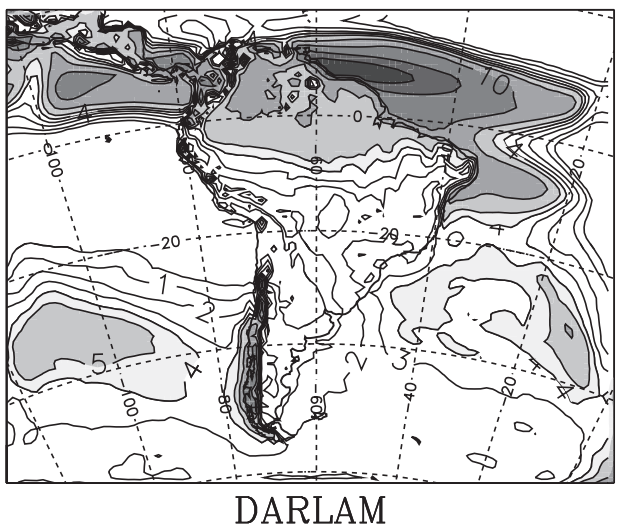

Figure 7. January daily precipitation (mm d^{-1}) from (a) *Xie and Arkin* [1997], (b) CSIRO Mk 2, and (c) DARLAM. Contour intervals are 0, 0.5, 1, 2, 3, 4, 5, 7, 10, and 15 mm d^{-1}; values higher than 4 mm d^{-1} are shaded.

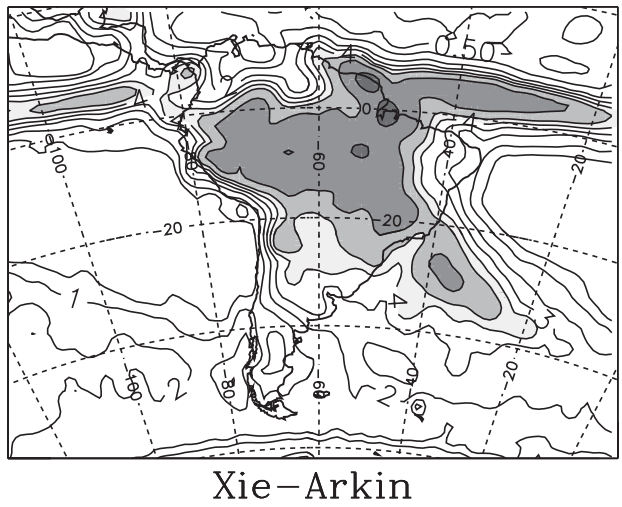

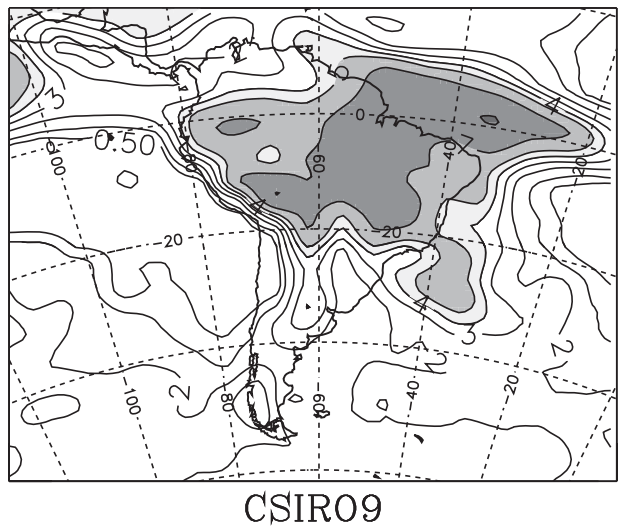

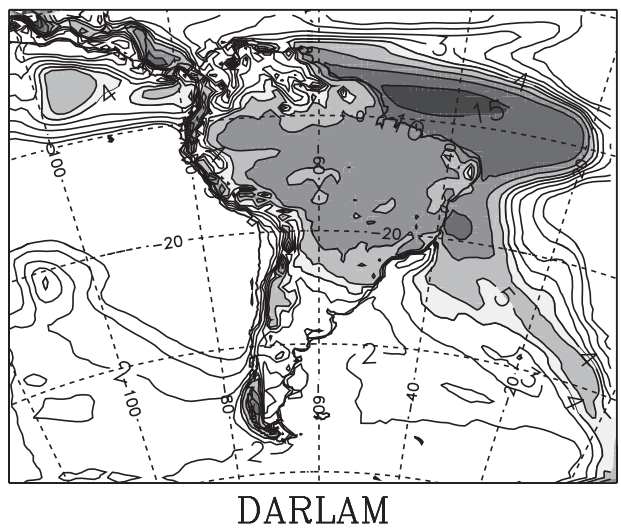

Figure 8. Same as in Figure 7, but for July.

Table 5. Spatial Pattern Correlation, Root Mean Square Error, and Overall Spatial Bias January Precipitation$^{1/3}$ for CSIRO Mk 2 and DARLAM, Compared to *Xie and Arkin* [1997][a]

		Pattern Correlation		RMS, (mm d^{-1})$^{1/3}$		Bias, (mm d^{-1})$^{1/3}$	
	N	GCM	DARLAM	GCM	DARLAM	GCM	DARLAM
Sea	7326	0,72	0,66	0,90	0,98	1,19	1,20
Continent	1687	0,70	0,67	1,13	1,20	1,64	1,70
Amazonia	534	0,78	0,73	1,23	1,27	1,83	1,86
Mountain	500	0,53	0,46	1,01	1,05	1,40	1,42
RP Basin	193	0,54	0,81	0,95	1,11	1,45	1,60
B Plateau	382	0,42	0,43	1,25	1,35	1,84	1,95

[a] RMS, root mean square; *N* is the number of DARLAM grid points; the subregions are defined in section 2.

one located west of Chile and the other, stronger jet located downstream of Argentina.

[36] It is clear that DARLAM represents the anticyclonic circulation much better than CSIRO Mk 2, with its center positioned at around 20°S, 60°W (compare Figure 9b with Figure 9c). Both the Bolivian High and the northeast trough are slightly displaced to the east with respect to ERA depiction. This shift may be explained by the DARLAM misrepresentation of the Amazonian precipitation; that in turn may be caused by a failure to reproduce the location of the Amazonian convective heat source. The GCM captures the location of the jet stream very well (Figure 9b) and also the two maxima, although their magnitudes are weak. DARLAM (Figure 9c) has better magnitudes than the GCM, but the two maxima are less clearly defined.

[37] During July (Figure 10a), the jet stream axis has shifted northward to ~35°S, except east of South America where a broad region of winds greater than 35 m s^{-1} extends from 30°S to 50°S. There is still a suggestion of a maximum over the Pacific, a minimum over South America and a weak second maximum over the Atlantic, although the differences are much less than for January.

[38] The jet stream is reasonably well simulated over the Pacific in both the GCM (Figure 10b) and DARLAM (Figure 10c), with better magnitudes in DARLAM. However, over South America and especially over the Atlantic Ocean, the jet stream is located too far north (by ~20°). Some of the differences during July can be attributed to the relative location of the subtropical and polar jets in the vertical. The models emphasize the subtropical jet at this level, while the analyses suggest equal strengths for the subtropical and polar jets. DARLAM also represents the wind direction and strengths over northern South America better than the GCM.

4.5. Low-Level Winds

[39] The low-level (sigma = 0.7) ERA meridional wind component field during January (Figure 11a) depicts two maxima between the Equator and 30°S. The one located around 15°S, 63°W is related to the trade winds crossing the Equator, curving anticyclonically and becoming northwesterly just to the east of the Andes, between the Bolivian Plateau and southern Amazonia. With a weak cyclonic gyre evident around 25°S, 65°W, this low-level flow turns more northerly south of 20°S and is an important source of water vapor transport from the Amazon Basin into the central plains of Argentina, southern Brazil, and Uruguay. The second wind maximum located around 25°S, 38°W is related to the SACZ [*Nogués-Paegle and Mo*, 1997].

[40] CSIRO Mk 2 (Figure 11b) weakly represents the anticyclonic turning of the trade winds with a maximum in the northerly component over Brazil, north of the ERA position. DARLAM (Figure 11c) locates the maximum just to the east of the mountains but overestimates it and does not extend it downwind of the central Andes. Further south, the flow progresses eastward instead of turning cyclonically to the south as depicted by the ERA field.

[41] As already mentioned, DARLAM produces less than normal observed precipitation in the Amazon and central Andes. *Lenters and Cook* [1997] discuss the breaking down of the full linear response of the Bolivian High to the condensational heating forcing associated with the Amazon Basin, the SACZ and the central Andes. Also, *Gandu and Geisler* [1991] relate the southward wind turning at 15°S to the presence of a thermal surface low located to the east of the Andes at 15°S, which they associated with a prescribed Amazon Basin heating. The inadequate simulation of the January mean low-level circulation pattern by DARLAM is consistent with its weak representation of the thermal low to the east of the Andes, and a shifted position of the Bolivian High. Both behaviors are consistent with the reduced simulated precipitation over western Amazonia and the central Andes. The maximum wind speed related to SACZ is well represented by both models and is slightly displaced northward, in accordance with the precipitation behavior in this region.

Table 6. Same as for Table 5, but for July

		Pattern Correlation		RMS, (mm d^{-1})$^{1/3}$		Bias, (mm d^{-1})$^{1/3}$	
	N	GCM	DARLAM	GCM	DARLAM	GCM	DARLAM
Sea	7326	0,67	0,58	1,00	1,06	1,33	1,33
Continent	1687	0,71	0,61	0,88	1,09	1,18	1,40
Amazonia	534	0,71	0,71	1,06	1,33	1,47	1,78
Mountain	500	0,86	0,76	0,89	1,00	1,20	1,28
RP Basin	193	−0,06	0,52	0,56	0,55	0,88	0,90
B Plateau	382	0,26	−0,11	0,68	1,03	0,86	1,29

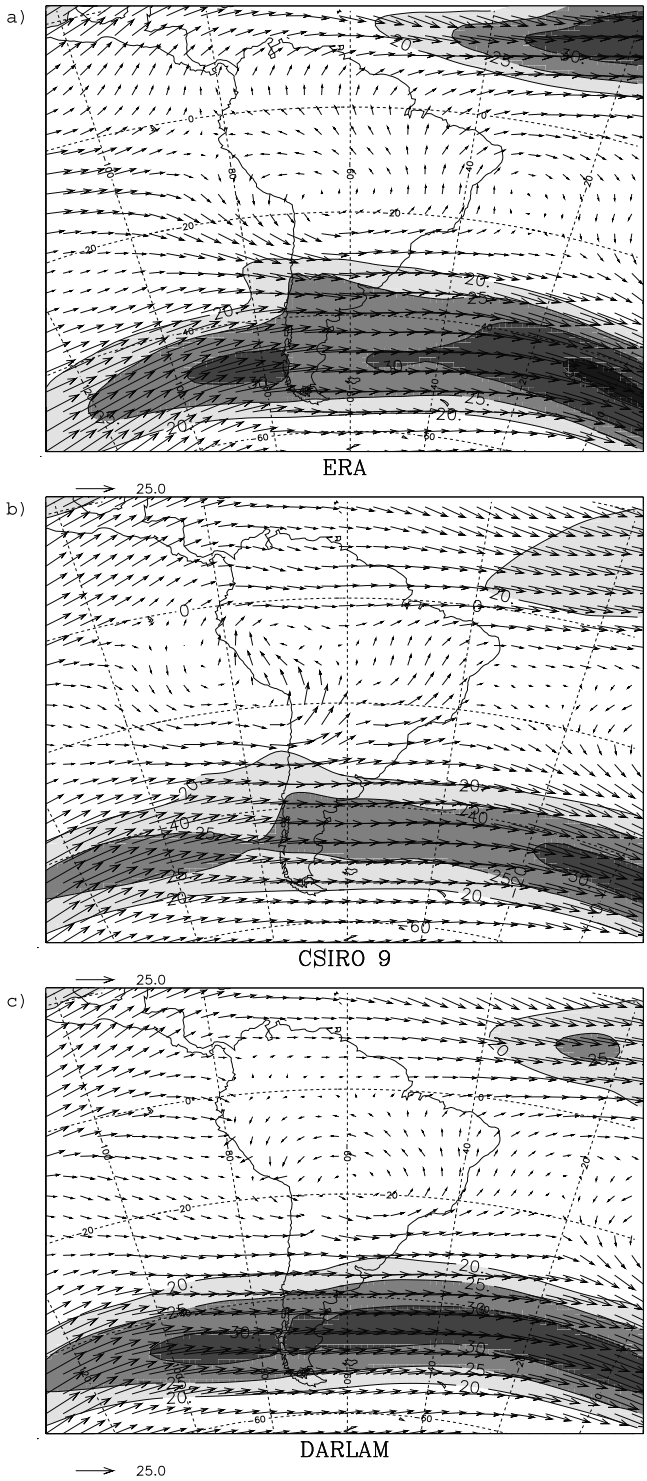

Figure 9. January wind vectors (m s^{-1}) and Zonal wind component at 0.10 sigma level for (a) ERA, (b) CSIRO Mk 2, and (c) DARLAM. Zonal wind component is shaded every 5 m s^{-1} for values higher than 20 m s^{-1}.

[42] The low-level wind field during July in ERA (Figure 12a) shows a maximum associated with the trades along the northeastern Brazil coast and a second, stronger maximum of northeasterly flow near 25°S, 55°W. This second maximum is associated with the westward displacement of the South Atlantic Subtropical Anticyclone during winter and consequently with an intensification of northerlies east of the Andes. The related moisture transport from low latitudes is however weaker than that during summer, as July is the time when the dry season is better defined.The GCM does not capture these observed features very well (Figure 12b), with only a weak onshore maximum over northeast Brazil and no maximum evident around 25°S, 55°W. DARLAM (Figure 12c) better captures the wind maximum at 25°S, 55°W, although the magnitude is still less than observed. The onshore flow over northeast Brazil is slightly weaker

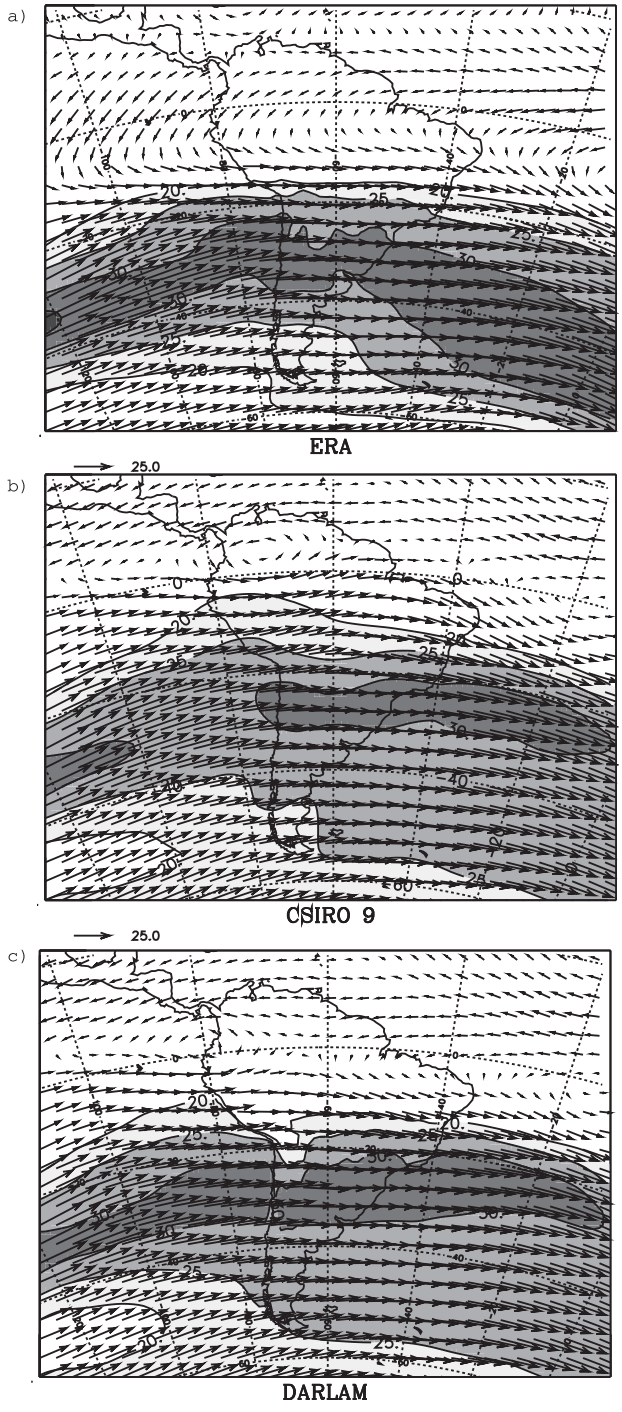

Figure 10. Same as in Figure 9, but for July.

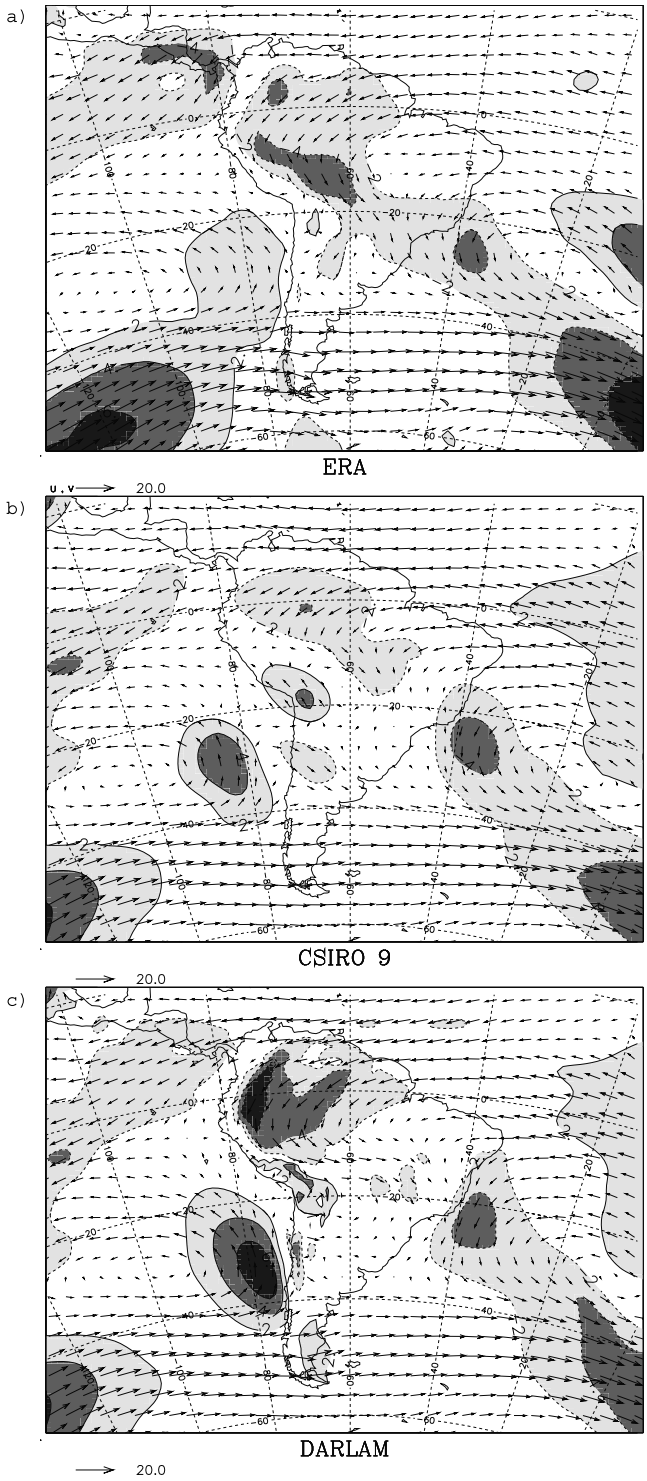

Figure 11. January wind vectors and meridional wind component at 0.70 sigma level for (a) ERA, (b) CSIRO Mk 2, and (c) DARLAM. Meridional wind component is shaded every 2 m s^{-1} for magnitudes exceeding 2 m s^{-1}; negative values are contoured with dashed lines and positive values with solid lines.

and therefore worse than the GCM. With the better depiction of the winds over central South America by DARLAM and associated better moisture transport and convergence, the rainfall over southeastern Brazil is also better represented, whereas the GCM lacks any rainfall maximum in this region.

5. Concluding Remarks

[43] The goal of this study was to test the capability of the CSIRO Mk 2-DARLAM nested modeling system for simulating January and July climate in the South American region. Further, it was desired to investigate over various

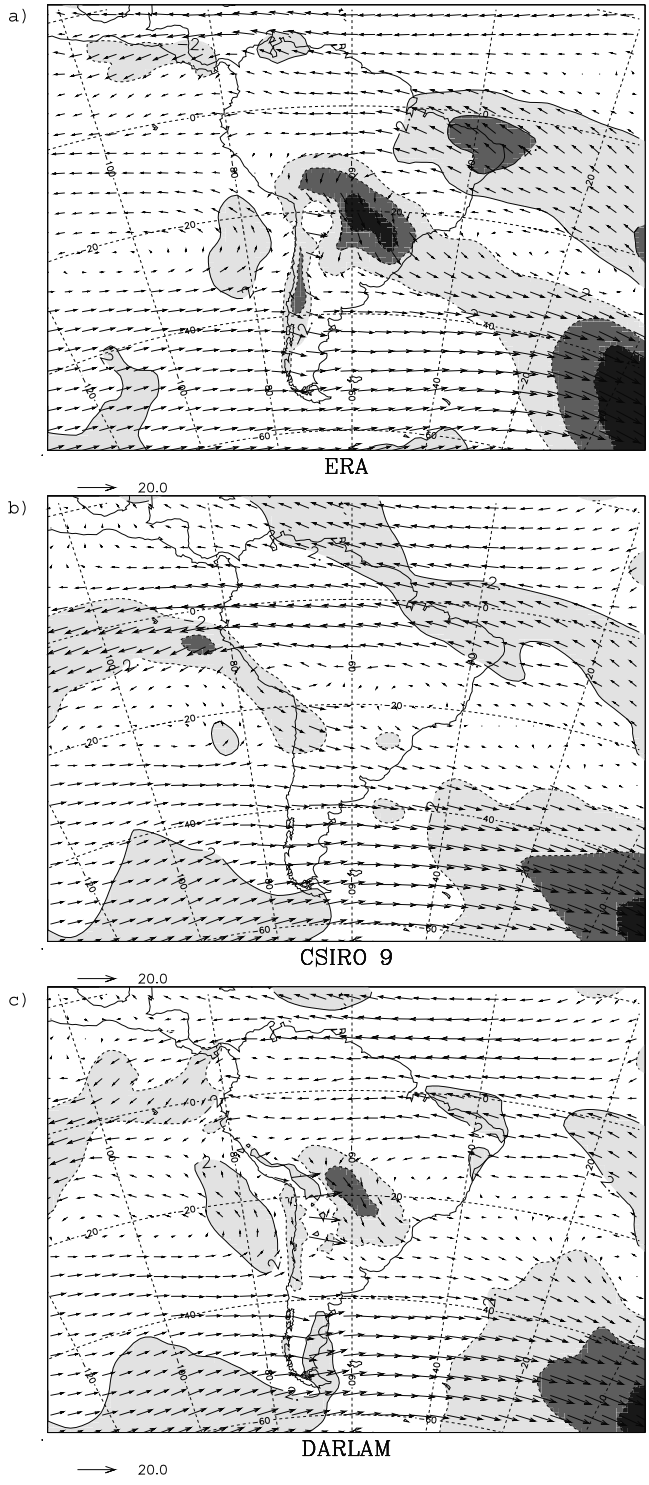

Figure 12. Same as in Figure 11, but for July.

subregions whether the finer horizontal resolution of DARLAM improves the simulation of the South American climate compared with CSIRO Mk 2.

[44] As expected, the simulated fields produced by the one-way nesting system provided a better representation of the South American climate when compared with that of the GCM. In particular, significant improvements have been found in the nested model climatology for near-surface temperature and mean sea level pressure. The DARLAM high-level wind pattern simulated the Bolivian High reasonably well, whereas CSIRO Mk 2 was not able to reproduce it.

[45] The Andes steep orography leads to excessive DARLAM monthly precipitation, especially between 25°S and 35°S. This problem has been also found in other geographical areas where a similar nesting approach has been used [*Jenkins and Barron*, 1997; *McGregor and Walsh*, 1994; *Giorgi et al.*, 1994; *Menendez et al.*, 2000].

[46] A comparison of January and July climate simulations shows a better wintertime performance. The January low-level flow and precipitation simulation deficiencies have been discussed in terms of the position and intensity of convective heating sources. A correct representation of these features may require an improvement in the convective and radiation parameterizations that are currently similar in both CSIRO Mk 2 and DARLAM. It should also be noted that inadequacies in the land surface scheme may lead to misrepresentation of boundary layer temperature and moisture and thus to inadequate triggering of convection.

[47] Simulation of present-day climate will also be enhanced by the availability of better data sets for SST, surface albedo, surface roughness, and vegetation characteristics. Another factor to be considered is the poor observational precipitation coverage in some areas over South America that introduces an uncertainty in the model-data comparison of South America climate description. Increased computer power, probably involving massively parallel computers, will allow longer simulations with better resolution. It should also become possible to perform two-way nested climate simulations or variable resolutions simulations over the whole globe.

[48] **Acknowledgments.** The authors would like to thank the two anonymous reviewers for their comments to help to clarify the paper. The ERA reanalyses were kindly provided by CPTEC under the LBA project (Large Scale Biosphere-Atmosphere Experiment in Amazonia). Project TX30 of the University of Buenos Aires, PICT 01757 of the Agencia Nacional de Promoción Científica y Tecnólogica and PIP 4520/96 of CONICET have partially funded this research. The authors would also like to thank Eva Kowalczyk for her contributions to development of the land surface scheme.

References

Arakawa, A., Design of the UCLA general circulation model. Numerical simulation of the weather and climate, *Tech. Rep. No. 7*, Dept. of Meteorol., Univ. of California, Los Angeles, Calif., 1972.

Carril, A., C. Menéndez, and M. Nuñez, Climate change scenarios over the South American region: An intercomparison of coupled general atmosphere—Ocean circulation models, *Int. J. Clim.*, *17*, 1613–1633, 1997.

Chou, S. C., A. M. B. Nunes, and I. F. A. Cavalcanti, Extended range forecast over South America using the regional eta model, *J. Geophys. Res.*, *105*, 10,147–10,160, 2000.

Davies, H., A lateral boundary formulation for multi-level prediction models, *Q. J. R. Meteorol. Soc.*, *102*, 405–418, 1976.

Dickinson, R. E., R. M. Errico, F. Giorgi, and G. T. Bates, A regional climate model for the western U.S., *Clim. Change*, *15*, 383–422, 1989.

Dorman, J. L., and P. J. Sellers, A global climatology of albedo, roughness length and stomatal resistance for atmospheric general circulation models as represented by the simple biosphere model (SiB), *J. Appl. Meteorol.*, *28*, 833–855, 1989.

Figueroa, S. N., P. Satyamurty, and P. L. Silva Dias, Simulations of the summer circulation over the South American region with an eta coordinate model, *J. Atmos. Sci.*, *52*, 1573–1584, 1995.

Gandu, A., and J. E. Geisler, A primitive equations model study of the effect of the topography on the summer circulations over tropical South America, *J. Atmos. Sci.*, *48*, 1822–1836, 1991.

Gandu, A., and P. L. Silva Dias, Impacts of tropical heat sources on the South American tropospheric upper circulation and subsidence, *J. Geophys. Res.*, *103*, 6001–6015, 1998.

Gibson, J. K., P. Kallberg, and S. Uppala, The ECMWF ReAnalysis (ERA) Project, *ECMWF Newsl.*, *73*, 7–17, 1996.

Gibson, J. K., P. Kallberg, S. Uppala, A. Hernandez, A. Nomura, and E. Serrano, ECMWF ReAnalysis Project Rep. Ser. 1, 72 pp., Eur. Cent. for Medium-Range Weather Forecast, Reading, U. K., 1997.

Giorgi, F., Simulation of regional climate using a limited area model nested in a general circulation model, *J. Clim.*, *3*, 941–963, 1990.

Giorgi, F., and M. R. Marinucci, Validation of a regional atmospheric model over Europe: Sensitivity of wintertime and summertime simulations to selected physics parametrization and lower boundary conditions, *Q. J. R. Meteorol. Soc.*, *117*, 1171–1206, 1991.

Giorgi, F., and M. R. Marinucci, An investigation of the sensitivity of simulated precipitation to model resolution and its implications for climate studies, *Mon. Wea. Rev.*, *124*, 148–166, 1996a.

Giorgi, F., and M. R. Marinucci, Improvements in the simulation of surface climatology over the European region with a nested modeling system, *Geophys. Res. Lett.*, *23*, 273–276, 1996b.

Giorgi, F., M. R. Marinucci, and G. Visconti, Use of a limited area model nested in a general circulation model for regional climate simulation over Europe, *J. Geophys. Res.*, *95*, 18,143–18,431, 1990.

Giorgi, F., M. R. Marinucci, and G. Visconti, A 2XCO2 climate change scenario over Europe generated using a limited area model nested in a general ciculation model, 2, Climate change scenario, *J. Geophys. Res.*, *97*, 10,011–10,028, 1992.

Giorgi, F., C. S. Brodeur, and G. T. Bates, Regional climate change scenarios over the United States produced with a nested regional climate model, *J. Clim.*, *7*, 375–399, 1994.

Jenkins, G. S., and E. J. Barron, Global climate model and coupled regional climate model simulation over the eastern United States: GENESIS and RegCM2 simulations, *Global Planet. Change*, *15*, 3–32, 1997.

Joubert, A., J. J. Katzfey, J. L. McGregor, and K. C. Nguyen, Simulating midsummer climate over Southern Africa using a nested regional climate model, *J. Geophys. Res.*, *104*, 19,015–19,025, 1999.

Kalnay, E., et al., NCEP/NCAR 40-year reanalysis project, *Bull. Am. Meteorol. Soc.*, *77*, 437–471, 1996.

Katz, R. W., Role of statistics in the validation of general circulation models, *Clim. Res.*, *2*, 35–45, 1992.

Labraga, J. C., The climate change in South America due to a doubling in the CO_2 concentration: Intercomparison of general circulation models equilibrium experiments, *Int. J. Clim.*, *17*, 377–398, 1997.

Lenters, J., and H. Cook, On the origin of the Bolivian High and related circulation features of the South American climate, *J. Atmos. Sci.*, *54*, 656–677, 1997.

Liebmann, B., G. N. Kiladis, J. A. Marengo, T. Ambrizzi, and J. D. Glick, *Submonthly Convective Variability over South America and the South Atlantic Convergence Zone*, *J. Clim.*, *12*, 1877–1891, 1999.

Louis, J.-F., A parametric model of vertical eddy fluxes in the atmosphere, *Bound. Layer Meteorol.*, *17*, 187–202, 1979.

McGregor, J. L., Accuracy and initialization of a two-time-level split semi-Lagrangian model, in *Short and Medium–Range Numerical Weather Prediction*, edited by T. Matsuno, pp. 233–246, Meteorol. Soc. of Jpn., Tokyo, 1987.

McGregor, J. L., Regional climate modelling, *Meteorol. Atmos. Phys.*, *63*, 105–117, 1997.

McGregor, J. L., and K. Walsh, Nested simulations of perpetual January climate over the Australian region, *J. Geophys. Res.*, *98*, 23,283 –23,290, 1993.

McGregor, J. L., and K. Walsh, Climate change simulations of Tasmanian precipitation using multiple nesting, *J. Geophys. Res.*, *99*, 20,889–20,905, 1994.

Menéndez, C., C. Saulo, and L. Li, Simulation of South American wintertime climate with a nested modelling system, *Clim. Dyn.*, *17*, 219–231, 2000.

Minetti, J., and W. Vargas, Behavior over South America in the periphery of the subtropical anticyclone, First Part (in spanish), *Meteorologica*, *14*, 645–656, 1983.

Nogués-Paegle, J., and K. C. Mo, Alternating wet and dry conditions over South America during summer, *Mon. Wea. Rev.*, *125*, 279–291, 1997.

Renwick, J. A., J. J. Katzfey, K. C. Nguyen, and J. L. McGregor, Regional model simulations of New Zealand climate, *J. Geophys. Res.*, *103*, 5973–5982, 1998.

Schwerdtfeger, W., (Ed.), *Climates of Central and South America*, *World Surv. Climatol.*, vol. 12, 522 pp., Elsevier Sci., New York, 1976.

Stidd, C. K., Cube-root normal precipitations distributions, *Trans. AGU*, *34*, 31–35, 1953.

Walsh, K., and J. L. McGregor, January and July climate simulations over the Australian region using a limited area model, *J. Clim.*, *8*, 2387–2403, 1995.

Walsh, K., and J. L. McGregor, Simulations of Antarctic climate using a limited area model, *J. Geophys. Res.*, *101*, 19,093–19,108, 1996.

Watterson, I. G., M. R. Dix, H. B. Gordon, and J. L. McGregor, The CSIRO nine level atmospheric general circulation model and its equilibrium present and doubled CO_2 climates, *Aust. Meteorol. Mag.*, *44*, 111–125, 1995.

Xie, P., and P. A. Arkin, Global precipitation: A 17-year monthly analysis based on gauge observations, satellite estimates, and numerical model outputs, *Bull. Am. Meteorol. Soc.*, *78*, 2539 –2558, 1997.

J. J. Katzfey and J. L. McGregor, Division of Atmospheric Research, CSIRO, Private Bag No. 1, Aspendale, Victoria 3195, Australia.

M. Nicolini, P. Salio, and A. C. Saulo, Departamento de Ciencias de la Atmósfera y los Océanos, Ciudad Universitaria, Pabellón 2, 2 Piso, (1428) Buenos Aires, Argentina. (nicolini@at1.fcen.uba.ar)